Surfactant-templated Synthesis of Resorcinol–Formaldehyde Polymer and Carbon Nanostructures: Nanospheres and Nanowires

Daisuke Fujikawa,[1] Masafumi Uota,[2] Takumi Yoshimura,[1] Go Sakai,[1] and Tsuyoshi Kijima*[1]
[1] *Department of Applied Chemistry, Faculty of Engineering, Miyazaki University, Miyazaki 889-2192*
[2] *CREST, Japan Science and Technology Cooperation, 4-1-8 Honcho, Kawaguchi 332-0012*

(Received February 6, 2006; CL-060154; E-mail: t0g102u@cc.miyazaki-u.ac.jp)

Thermosetting polymer nanospheres and nanowires have been synthesized by the NaOH-catalyzed polymerization of resorcinol and formaldehyde in the presence of cetyltrimethylammonium bromide as a core template together with/without trimethylbenzene as an additive and topotactically converted into their carbonized forms.

Outstanding attention is currently focused on nano-sized or nano-structured carbons for their various applications such as electrodes for batteries and fuel cells, electric double layer capacitors, and catalyst supports.[1–4] Solid-templating approach has been widely used for the synthesis of a variety of highly ordered nanoporous or nanofibrous carbons.[1c,5] In contrast, the surfactant-templating approach, which was first developed for the synthesis of mesoporous silica,[6] has been much less applied to the synthesis of nanocarbons.

Thermosetting resorcinol (R)–formaldehyde (F) resins were extensively applied to the synthesis of nanometer-sized spherical cross-linked RF polymer and carbon gels.[7] Highly ordered mesoporous carbons were also prepared through the RF reaction within copolymer nanoassemblies reorganized in nonaqueous solvent.[8] Nishiyama et al. performed the RF polymerization reaction using sodium carbonate as a catalyst in the presence of cationic surfactant, which yielded only microporous spherical carbons of 1–3 µm diameter.[9] Nevertheless, the interaction between RF polymers and cationic surfactant molecules may be more finely tuned through the controlled ionization of phenolic hydroxyl groups as well as the use of some additives. Here, we report the synthesis of RF polymer nanowires 80–300 nm in diameter and their conversion into carbon nanowires of 40–150 nm diameter through the NaOH-catalyzed polymerization of R and F in the co-presence of cetyltrimethylammonium bromide (CTAB) and 1,3,5-trimethylbenzene (TMB). The TMB-free processes yield RF polymer nanospheres and microwires with a layered structure, as well as their topotactically carbonized materials.

In the typical fabrication process, R, CTAB, NaOH, TMB, and water were mixed at a 1:1:x:y:360 molar ratio ($x = 0.25$–1.0 and $y = 0$–1) to obtain a precursory solution. A mixed solution of R and F at a 1:4 molar ratio was added dropwise to the micellar solution at 50 °C with vigorous stirring. After being heated at 50 °C for 2 h and then at 90 °C for 72 h, the mixture was hydrothermally reacted with paraformaldehyde at 150 °C for 24 h. The total molar ratio of R, F, CTAB, NaOH, TMB, and H_2O was 2:4:1:x:y:360. The resulting products were washed with water and then dried at 60 °C.

The resulting solids markedly changed in morphology depending on the NaOH and TMB amounts added (Figures 1a–1f). In the TMB-free system, the reaction at the NaOH amount of as low as $x = 0.25$ yielded nanospheres of 250–400 nm diameter (Figure 1a). The TEM image of this sample showed a spherical aggregate of flaky materials (Figure 1b) and the broad XRD peak observed for the same sample suggested that the flaky materials have a layered structure with an inter-layer spacing of ca. 3.8 nm (Figure 2a). The RF polymer nano-spheres formed as an aggregate of nanosheets are in marked contrast to those obtained by the conventional surfactant-free RF sol–gel reactions: The latter are obtained as an aggregate of spherical but 3-dimensional (3D) cross-linked RF polymers.[7] The reaction at the NaOH amount of as high as $x = 1.0$ produced microwires with a diameter of 10–30 µm (Figure S1a) (S is referred to Supporting Information). The SEM image of the fracture surface of microwires exhibited a stripe pattern (Figure S1b) and the TEM image of their fragments showed the formation of laminated materials (Figure S1c). Both images are consistent with the XRD data indicating that the microwires have a layered structure with an interlayer spacing of ca. 3.6 nm (Figure 2b).

In the TMB-added ($y = 1.0$) system, the RF polymerization at $x = 0.25$ resulted in nanowires with a rounded cross section of as small as 80–300 nm diameter (Figures 1c and 1d). The length of the nanowires was estimated to be much more than 3 µm. Upon ultrasonication in ethanol after milling in liquid N_2, the wiry sample was exfoliated into nanosheets with a thickness of 10–15 nm and a width of 180–430 nm: The sheet widths were close to the circumference of nanowires or less (Figure 3). Furthermore, the broad XRD peak for the as grown nanowire sample suggested that the exfoliated sheets have a layered structure with an interlayer spacing of ca. 4.4 nm (Figure 2c). These findings indicate that the as grown nanowires might have a multi-cylindrical structure of polymer nanosheets with a curved but highly disordered layered structure. Actually, the specific layered structure is also consistent with the curved stripes observed for the cross section of spherulite particles 4–10 µm in diameter, which

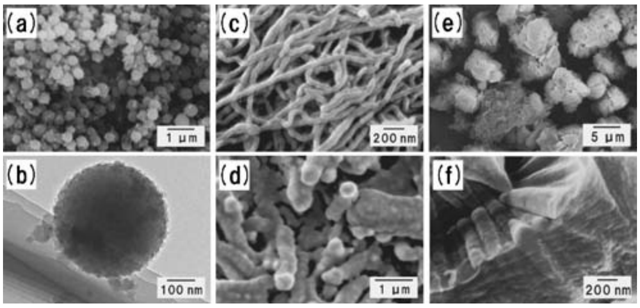

Figure 1. (a and c–f) SEM and (b) TEM images of the RF/CTA composites synthesized under various conditions: (a and b) $x = 0.25$, $y = 0$; (c and d) $x = 0.25$, $y = 1.0$; (e and f) $x = 0.5$, $y = 1.0$. The images (d) and (f) were obtained for the fracture surface of samples for (c) and (e), respectively.

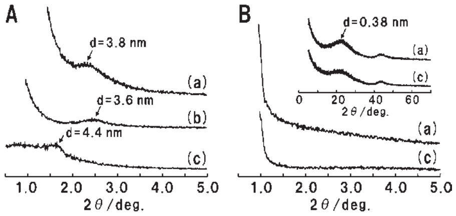

Figure 2. XRD patterns of the RF/CTAB composites (A) as grown and (B) calcined at 1000 °C in N_2 after acid-treatment: (a) $x = 0.25$, $y = 0$; (b) $x = 1.0$, $y = 0$; (c) $x = 0.25$, $y = 1.0$.

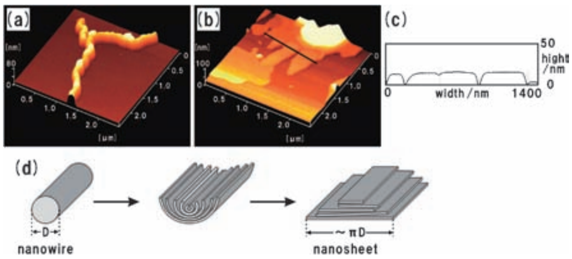

Figure 3. Tapping-mode AFM images of the RF/CTA composites obtained at $x = 0.25$, $y = 1.0$: (a) as grown, (b) ultrasonicated in ethanol after milling in liquid N_2, (c) the cross-sectional profile along the line in (b) and (d) a schematic model for the exfoliation of nanowire into nanosheets.

were formed at the intermediate NaOH amount of $x = 0.5$ and coexisted with nanowires (Figures 1e and 1f). The reaction at $x = 1.0$ produced feature-poor particles with a sheet-like appearance (Figure S1d).

All the as-grown solids were identified as a composite of RF polymer and CTA by their FT-IR spectra giving rise to strong bands attributable to CH_2 group at 2922 and 2855 cm^{-1}, along with the bands due to aromatic group at 1611 cm^{-1} (Figure S2a). The incorporation of CTA in the solids was also confirmed by a remarkable decrease of the former bands upon the removal of CTA species caused by the ion-exchange treatment with HCl in ethanol (Figure S2b). CHN elemental analysis showed that the N/C ratio for the as grown solids increases from 1.4 to 2.6% with an increase of x from 0.25 to 1.0 for the TMB-free system but remains nearly constant at ca. 1.8–2.0% for the other. This means that the incorporation of CTA species in the polymer matrix is promoted with an increase in electrostatic interaction between CTA^+ ions and anionized R species in the TMB-free system but it remains independent of x in the TMB-added system. The latter result would be obtained because the electrostatic interaction between both species is compensated by the hydrophobic one between the alkyl groups of CTA^+ and the TMB molecules added.

On calcination at 1000 °C for 4 h in N_2 after the acid-treatment the RF polymer composite nanospheres and nanowires were successfully converted into their carbon analogs 160–350 and 40–150 nm in diameter, respectively, with keeping their precursory morphologies (Figure 4A). The removal of surfactant species prior to calcination was essential for the topotactic carbonization. The slightly ordered layered structure for both composites became completely disordered through carbonization, but with the development of poorly ordered carbon layers ca. 0.4 nm in spacing (Figure 2B). The carbon nanospheres and nanowires thus formed were further identified as microporous materials with specific surface areas of 1599 and 757 $m^2\,g^{-1}$, micropore diameters of 0.7 and 0.6 nm, and micropore volumes of 0.61 and 0.31 $cm^3\,g^{-1}$, respectively, from their N_2 adsorption–desorption isotherms, pore size distribution curves and t-plots (Figure 4B and S3). The much larger surface area and pore volume for the former would be observed mostly because the nanosheets within the spherical polymers are more loosely packed than those in the other, leading to the formation of much more micropores through carbonization.

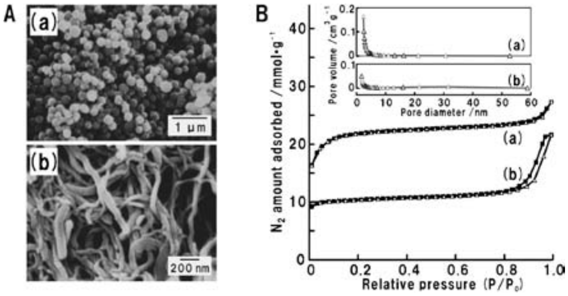

Figure 4. (A) SEM images and (B) N_2 adsorption–desorption isotherms and BJH pore size distribution curves of the carbonized materials obtained by calcination of acid-treated RF/CTAB composites at 1000 °C in N_2: (a) $x = 0.25$, $y = 0$; (b) $x = 0.25$, $y = 1.0$.

In conclusion, we first demonstrated a surfactant-templated route to synthesize RF polymer nanospheres and nanowires with a straight or curved layer structure, as well as their morphologically similar carbonized forms with high surface areas. The present approach successfully used NaOH as a combined source of catalyzing and ionizing agents, CTAB as a core templating agent, and TMB as a micellar structure modifier. This approach is based on controlling the interaction between RF polymers and cationic surfactant molecules through the ionization of phenolic hydroxyl groups of resorcinol species, along with the topotactic carbonization of nanostructured RF polymers through their excellent thermosetting character. Particularly, the additional use of TMB as a micelle modifier is highly effective for structurally modifying the polymer composites and their carbonized forms from nanospheres to nanowires.

This work was supported by Grant-in-Aid for the CREST of Japan Science and Technology Agency (JST) and JSPS Research Fellowships for Young Scientist.

References

1 a) M. Inagaki, L. R. Radovic, *Carbon* **2002**, *40*, 2279. b) M. Inagaki, K. Kaneko, T. Nishizawa, *Carbon* **2004**, *42*, 1401. c) J. Lee, S. Han, T. Hyeon, *J. Mater. Chem.* **2004**, *14*, 478.

2 S. H. Joo, S. J. Choi, I. Oh, J. Kwak, Z. Liu, O. Terasaki, R. Ryoo, *Nature* **2001**, *412*, 169; T. Heyeon, S. Han, Y.-E. Sung, K. W. Park, Y. W. Kim, *Angew. Chem., Int. Ed.* **2003**, *42*, 4352.

3 M. Toyoda, Y. Tani, Y. Soneda, *Carbon* **2004**, *42*, 2833; J. Lee, S. Yoon, S. M. Oh, C. H. Shin, T. Hyeon, *Adv. Mater.* **2000**, *12*, 359.

4 J. Lee, S. Han, H. Kim, J. H. Koh, T. Hyeon, S. H. Moon, *Catal. Today* **2003**, *86*, 141.

5 R. Fernández-Saavedra, P. Aranda, E. Ruiz-Hitzky, *Adv. Funct. Mater.* **2004**, *14*, 77.

6 C. T. Kresge, M. E. Leonowicz, W. J. Roth, J. C. Vartuli, J. S. Beck, *Nature* **1992**, *359*, 710; T. Yanagisawa, T. Shimizu, K. Kuroda, C. Kato, *Bull. Chem. Soc. Jpn.* **1990**, *63*, 988.

7 S. A. Al-Muhtaseb, J. A. Ritter, *Adv. Mater.* **2003**, *15*, 101.

8 C. Liang, K. Hong, G. A. Guiochon, J. W. Mays, S. Dai, *Angew. Chem., Int. Ed.* **2004**, *43*, 5785; C. Liang, K. Hong, G. A. Guiochon, J. W. Mays, S. Dai, *Angew. Chem.* **2004**, *116*, 5909.

9 N. Nishiyama, T. Zheng, Y. Yamane, Y. Egashira, K. Ueyama, *Carbon* **2005**, *43*, 269.

Published on the web (Advance View) March 18, 2006; DOI 10.1246/cl.2006.432